Metallomics

RSC Publishing

PAPER

View Article Online
View Journal | View Issue

Cite this: *Metallomics*, 2013, **5**, 1656

Profiling the iron, copper and zinc content in primary neuron and astrocyte cultures by rapid online quantitative size exclusion chromatography-inductively coupled plasma-mass spectrometry

Dominic J. Hare,[ab] Alexandra Grubman,[c] Timothy M. Ryan,[a] Amber Lothian,[a] Jeffrey R. Liddell,[c] Rudolf Grimm,[d] Toshiaki Matsuda,[e] Philip A. Doble,[b] Robert A. Cherny,[a] Ashley I. Bush,[a] Anthony R. White,[c] Colin L. Masters[a] and Blaine R. Roberts*[a]

Metals often determine the chemical reactivity of the proteins to which they are bound. Each cell in the body tightly maintains a unique metalloproteomic profile, mostly dependent on function. This paper describes an analytical online flow injection quantitative size exclusion chromatography-inductively coupled plasma-mass spectrometry (SEC-ICP-MS) method, which was applied to profiling the metal-binding proteins found in primary cultures of neurons and astrocytes. This method can be conducted using similar amounts of sample to those used for Western blotting (20–150 μg protein), and has a turnaround time of <15 minutes. Metalloprotein standards for Fe (as ferritin), Cu and Zn (as superoxide dismutase-1) were used to construct multi-point calibration curves for online quantification of metalloproteins by SEC-ICP-MS. Homogenates of primary neuron and astrocyte cultures were analysed by SEC-ICP-MS. Online quantification by external calibration with metalloprotein standards determined the mass of metal eluting from the column relative to time (as pg s^{-1}). Total on-column Fe, Cu and Zn detection limits ranged from 0.825 $\pm$ 0.005 ng to 13.6 $\pm$ 0.7 pg. Neurons and astrocytes exhibited distinct metalloprotein profiles, featuring both ubiquitous and unique metalloprotein species. Separation and detection by SEC-ICP-MS allows appraisal of these metalloproteins in their native state, and online quantification was achieved using this relatively simple external calibration process.

Received 21st August 2013,
Accepted 7th October 2013

DOI: 10.1039/c3mt00227f

www.rsc.org/metallomics

Introduction

The brain maintains some of the highest concentrations of metals in the body.[1] Free alkali and alkaline earth metals play important roles in the transmission of nerve impulses and signal transduction, whilst transition metals, including Fe, Cu and Zn mediate a variety of cellular functions by way of their unique redox chemistry. Concentrations of these metals in the brain range from 10 to 100 μM, depending on the organelle and cell type in which they are found,[2] and the brain must tightly regulate the chemical state of these transition metals to ensure oxidative stress *via* metal-mediated Fenton and Haber–Weiss-type chemistry is controlled. Increasing evidence has suggested improper transition metal metabolism may contribute to the pathogenesis of various neurological disorders, including Alzheimer's and Parkinson's disease, through generation of toxic reactive oxygen species by labile metal ions.[3]

The source of oxidative stress-inducing metal species is a continuous point of contention with regard to the brain. Fe, Cu and Zn are distributed throughout the brain in a highly compartmentalised manner,[4] reflective of the diverse roles metal species play across the most complex organ in the body. Indeed, metal distribution is likely to be equally distinct at the cellular level, both with regard to total metal content and the protein species to which they are bound.

As such, we set out to examine the distribution of Fe, Cu and Zn according to the molecular species in two of the major cell types found throughout the brain: neurons and astrocytes. Interactions between these cell types govern a huge amount

[a] *The Florey Institute of Neuroscience and Mental Health, The University of Melbourne, Kenneth Myer Building, 30 Royal Parade, Parkville, Victoria, 3052, Australia. E-mail: blaine.roberts@florey.edu.au; Tel: +61 3 9035 6635*
[b] *Elemental Bio-imaging Facility, University of Technology, Broadway, Sydney, New South Wales, Australia*
[c] *Centre for Neuroscience & Department of Pathology, The University of Melbourne, Parkville, Victoria, Australia*
[d] *Agilent Technologies, Santa Clara, California, USA*
[e] *Agilent Technologies, Tokyo, Japan*

of neurophysiological processes, from development to pathology; yet detailed study of the chemistry surrounding the relationship of these two integral cells has been somewhat limited by the lack of suitably sensitive analytical techniques. Rapid improvements to analytical technology have helped remove a key challenge to understanding both the nature of brain function and how it is compromised in disease. Cahoy *et al.*[5] recently applied both fluorescence-activated cell sorting and GeneChip Array technology to profile the transcriptome of neurons, astrocytes and oligodendrocytes, finding that the genetic characteristics of the latter two cell types were so markedly different that previous generic classification of them both as 'glia' is likely insufficient. Yang *et al.*[6] used a proteomic approach to characterise the diversity of chemical species in rat cerebellar neurons and astrocytes, identifying both concurrent and unique proteins in both cell types, presented in a reference database. Both studies identified a range of cellular markers that more distinctly differentiate astrocytes and neurons then the traditional glial fibrillary acidic protein (GFAP) marker.

Thus, there is little doubt that the metalloproteomic profile of neurons and astrocytes contains unique information regarding the host cell type. Further, proteins that have been implicated in neurological diseases have also been suggested to play roles in metal metabolism, such as the Zn and Cu interactions with prion protein (PrP)[7] and proposed role of ionic Zn and Cu in the aggregation of β-amyloid (Aβ) in Alzheimer's disease.[3,8] However, the ubiquity of trace metals (Fe, Cu and Zn in particular) in the cell, as well as the relatively weak intermolecular forces governing metal–protein ligands presents an analytical challenge to achieving separation and detection of physiologically-relevant species.[9–11] Only fractionation of complex biological mixtures, usually *via* chromatographic separation, can provide clues as to whether changes in metal levels observed in neurological tissues are global or confined to a particular protein, and this protocol must ensure that metal–protein ligands are preserved. Lelie *et al.*[12] recently used such an approach to show that Cu,Zn-superoxide dismutase (SOD-1) metallation status, specifically the absence of Cu, was an identifying feature of familial amyotrophic lateral sclerosis (ALS).

Here, we employed native separation using size exclusion chromatography (SEC) hyphenated to ICP-MS for detection of metal cofactors according to molecular weight of the eluting biomolecules. Coupling SEC to elemental detection itself is not a new analytical technique; the first featured examples, reported in the 1980s, used atomic absorption[13] and atomic emission spectrometry[14] to detect trace metals in various biological fluids. Since then, a number of examples of SEC hyphenated to mass specific detection have been used to study trace metals in a variety of physiological and disease states, including rat serum,[15] cancerous human thyroid tissue,[16] murine neurological tissue[17] and platinum-treated human blood products[18] to name just a few. Common themes to these foundation papers are lengthy runtimes and difficulties in acquiring truly quantitative data. Using standard metalloproteins, we were able to absolutely quantify the metal content of each eluting species, and have suggested the possible biological molecules associated with specific metal ions. We present a method that is well suited to high throughput analysis of biological samples relevant to the emerging field of metalloproteomics[19] using minimal sample volumes and rapid chromatographic separations.

Experimental

Chemicals and standards

SOD-1 (Cu,Zn) and ferritin (Fe; Sigma Aldrich, Castle Hill, Australia) protein standards were used for metal quantification. Ammonium nitrate buffers were prepared fresh daily using MiliQ (18.2 MΩ) H_2O. All samples undergoing solution ICP-MS analysis for bulk metal content were diluted to volume in 1% (v/v) Suprapur HNO_3. SEC column calibration was performed using molecular weight standards for ferritin (M_W = 450 kDa), ceruloplasmin (M_W = 151 kDa), conalbumin (M_W = 75 kDa; GE Healthcare, Rydalmere, Australia), SOD-1 (M_W = 32 kDa (dimer)) and metallothionein IIa (M_W = 6.5 kDa).

Liquid chromatography-inductively coupled plasma-mass spectrometry

We used an Agilent Technologies 1200 liquid chromatography system (Mulgrave, Australia) with the eluent directly inserted into a standard perfluoroalkoxy (PFA) concentric design nebuliser *via* polyethyl ether ketone (PEEK) tubing (o.d. 1.58 mm; i.d. 0.13 mm). The nebuliser was fitted to an Agilent Technologies 7700x ICP-MS. Helium was used as a collision gas to remove polyatomic interferences. Separations were performed on an Agilent Technologies Bio-SEC 3 size exclusion column (3 μm particle size; 150 Å pore structure; 4.6 mm i.d.) with a 200 mM ammonium nitrate buffer (pH 7.7–7.8). The ICP-MS was tuned daily using solution nebulisation of a 1 μg L^{-1} Li, Co, Y, Ce and Tl standard. Typical operating parameters of the SEC-ICP-MS system are given in Table 1.

External calibration

SOD-1 and ferritin standards were prepared fresh prior to analysis. Standards were reconstituted in 0.1 M phosphate

Table 1 Typical operational SEC-ICP-MS parameters

Agilent 1200 LC	
Mobile phase	0.2 M NH_4NO_3 (pH 7.7–7.8)
Column type	Agilent Bio-SEC 3
Particle size	3 μm
Pore size	150 Å
Flow rate	mL min^{-1}
Injection volume	1–100 μL (100 μg total protein)
Column dimensions	4.6 mm (i.d.) × 150 mm
Agilent 7700x ICP-MS	
RF power	1550 W
Sample depth	8.0 mm
Carrier gas	0.95 L min^{-1}
Makeup gas	0.20 L min^{-1}
Spray chamber temperature	7 °C
Extracts 1, 2	−12, −200 V
Omega bias, lens	−95, 8.3 V
Deflect, plate bias	2.2, −60 V
Cell entrance, exit	−38, −68 V
Octopole bias, RF	−18.0, 200 V
Collision gas	He, 3.4 mL min^{-1}

buffered saline (PBS) and total metal content was determined by bulk ICP-MS analysis. Total metal loading on column was controlled by varying the injection volume from 3 to 75 μL. The area under baseline-corrected peaks was integrated using Prism 5 (GraphPad, La Jolla, USA) and used to construct multi-point calibration curves for each measured mass. Linear regression analysis was used to convert signal intensity (counts per second) to picogram of metal per second.

Primary cell cultures

Primary murine culture protocols were approved by the University of Melbourne Biosciences Animal Ethics Committee (approval number 1011753.4). For primary cortical cultures, E14 mouse cortices were removed, dissected free of meninges and dissociated in 0.025% trypsin. Viable dissociated cells were suspended in Minimum Eagle's Medium supplemented with 10% fetal bovine serum, 5% horse serum, 1% glutamine, and 10 μg mL^{-1} gentamicin, plated into poly-L-lysine coated 6 well culture plates (1.5×10^6 cells per well), and incubated at 37 °C in 5% CO_2. Growth medium was replaced with Neurobasal growth medium supplemented with 2% B27, 1% glutamine and 10 μg mL^{-1} gentamicin the following day. 3–4 days after plating, half of the media was replaced with fresh Neurobasal media. Cells were used for experiments 6 days after plating.

For astrocyte cultures, neonatal mice were decapitated and whole brains were removed and placed into ice-cold preparation buffer (containing 8 g L^{-1} NaCl, 400 mg L^{-1} KCl, 30 mg L^{-1} KH_2PO_4, 24 mg L^{-1} Na_2HPO_4, 20 g L^{-1} sucrose, 1 g L^{-1} glucose, 200 U mL^{-1} penicillin and 200 μg mL^{-1} streptomycin). Brains were sequentially passed through 250 μm and 135 μm gauze and centrifuged at 500 *g* for 5 min. Cell pellets were resuspended in growth medium (high glucose DMEM containing 10% fetal bovine serum, 50 U mL^{-1} penicillin and 50 μg mL^{-1} streptomycin) and plated in 6 well plates at 1.5×10^6 cells per well. Cells were maintained at 37 °C with 10% CO_2. Growth medium was replaced at 7 and 14 days, and experiments were performed after 16 days *in vitro*.

Sample preparation and analysis

Pellets of cultured neurons and astrocytes were resuspended in Tris-buffered saline (TBS; 50 mM Tris, 150 mM NaCl; pH 8.0) with added EDTA-free protease inhibitors (Roche, Castle Hill, Australia) and homogenized by 6 passes through a 26-gauge needle. The homogenate was then centrifuged at 13 200g for 5 minutes and the supernatant recovered. Injection volumes were standardised according to total protein content (UV absorbance at 280 nm) of the sample (*ca.* 10 μg μL^{-1}) measured by a NanoDrop spectrophotometer (ThermoFisher Scientific, Victoria, Australia). Samples were kept at 4 °C prior to injection using a Peltier-cooled autosampler. Each injection contained approximately 100 μg of total protein.

Results and discussion

Analytical performance

External calibration using multiple injections of metalloproteins standards enabled us to quantify both the total metal content in individual SEC-ICP-MS separations and the eluting metal concentration in pg s^{-1}.[20] Injection volumes ranged from 3 to 75 μL, for effective loading of 6–150 ng of Fe and 0.6–15 ng of Cu and Zn, which was in turn used to perform external calibration by linear regression with good linearity ($r^2 > 0.999$) for the three measured masses (Fig. 1a–c). Limits of analysis were determined using 3σ for limit of detection (LOD) and 10σ for limit of quantification (LOQ) for total metal loaded on column. For Fe, LOD and LOQ were 0.825 ± 0.005 ng and 2.75 ± 0.02 ng, respectively, equivalent to 14.8 ± 0.1 pmoles and 49.2 ± 0.4 pmoles. Cu and Zn returned LOD and LOQ values of 130 ± 22 pg (2.05 ± 0.35 pmoles) and 433 ± 74 pg (6.81 ± 1.16 pmoles); and 13.6 ± 0.7 pg (0.21 ± 0.01 pmoles) and 45.6 ± 2.4 pg (0.70 ± 0.04 pmoles), respectively. Repeated injections of 20 ng Fe (as ferritin) and 2.0 ng Cu and Zn (as SOD-1) ($n = 4$) returned coefficients of variation of 1.28%, 7.26%, and 2.40%. Calibration of the SEC column using Fe-, Cu- and Zn-binding metalloproteins returned good linearity for unknown molecular weight determination (Fig. 1d).

This quantitative SEC-ICP-MS method is well suited to high throughput analysis. The smaller column diameter (4.6 mm) than previous SEC-ICP-MS methods allows for smaller injection volumes (1–100 μL per injection) while maintaining sensitivity and reduced turnaround time per sample (<15 min).

Quantification of metal content of neurons and astrocytes

Chromatograms for each measured mass were normalised to the total peak area of the 280 nm absorbance trace (in addition to pre-injection standardisation using absorbance at 280 nm measured by UV-Vis spectroscopy), and thereby total protein content to confirm equivalent mass loading onto the SEC column. The total peak area for each measured mass was used to determine the total metal loading on column, and thus the concentration of metal in the homogenate per 1 mg of total protein loaded (Table 2). This approach allows for both speciation of metalloproteins and assay of the total metal content of cells. Interestingly, the total Fe content of both neuronal and astrocytic cultures was lower than Cu and Zn, even though Fe is generally at a higher concentration in brain tissue,[21] suggesting that either high brain Fe is sourced from other cell types, such as Fe-rich oligodendrocytes,[22] or that typical cell culturing conditions are Fe-deficient. In fact, we have previously observed that increase in astrocyte uptake of free Fe in metal-enriched (as ferric ammonium citrate; FAC) was as much as 20-fold,[23] while cellular uptake of ionic Cu and Zn was minimal.[24,25] The Fe content of both cell types was comparable to previously reported values using alternative quantitative techniques, such as the ferrozine-based colourimetric assay[26] and atomic absorption spectroscopy.[27] Similarly, the Cu content of astrocytes[28] and neurons[29] was also analogous to previous reports, as was the basal level of Zn in both cell types compared to other cell culture studies.[30,31] In general, astrocytes contained a greater concentration of both Fe and Zn than neurons, while neurons contained around twice the Cu concentration to that of astrocytes.

The method presented here demonstrates several significant advances in LC-ICP-MS separation and detection. Quantification of eluting metals has previously required bulk assay of

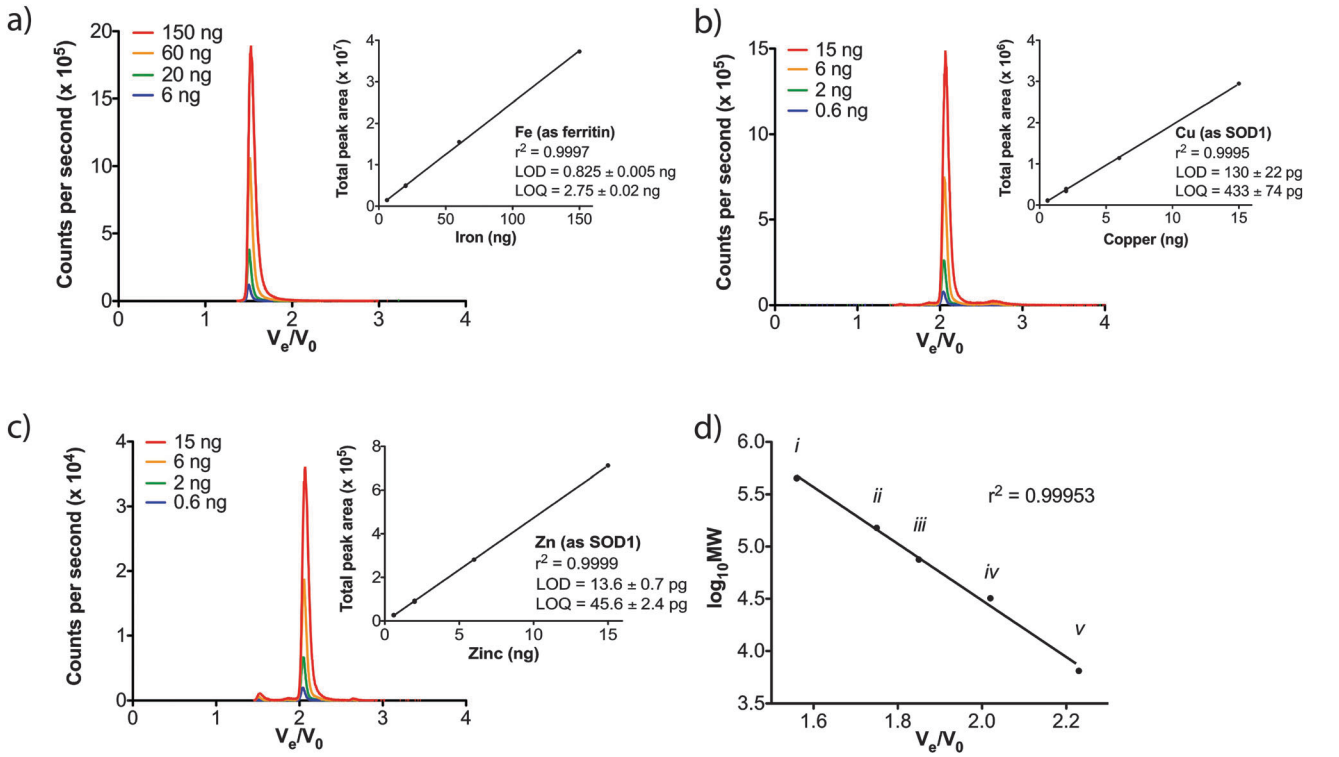

Fig. 1 External calibration procedure for (a) Fe, (b) Cu and (c) Zn by SEC-ICP-MS. Total metal injected onto the SEC column was controlled by increasing the injection volume of a known metalloprotein standard (ferritin for Fe; SOD-1 for Cu and Zn). Integration of the total area under curve (AUC) for each injection was used to perform linear regression analysis against the total metal injected, allowing conversion of ICP-MS signal output to pg s^{-1}. (d) SEC column was calibrated using ferritin (i; M_W = 450 kDa), ceruloplasmin (ii; M_W = 151 kDa), conalbumin (iii; M_W = 75 kDa), SOD-1 (iv; M_W = 32 kDa) and metallothionein IIa (v; M_W = 6.5 kDa).

Table 2 Fe, Cu and Zn concentration (per mg total protein) in neuron and astrocyte cultures

	Neurons (n = 4)		Astrocytes (n = 5)	
	ng mg^{-1}	nmol mg^{-1}	ng mg^{-1}	nmol mg^{-1}
Fe	7.31 ± 0.90[a]	0.131 ± 0.016[a]	27.7 ± 2.0[a]	0.497 ± 0.037[a]
Cu	200 ± 30	3.15 ± 0.47	105 ± 9	1.66 ± 0.14
Zn	29.1 ± 3.8	0.445 ± 0.058	47.7 ± 3.3	0.730 ± 0.050

[a] Below limit of quantification, indication only.

collected fractions,[32] which further weakens the already poor separation resolution experienced with native SEC separation. Online quantification *via* flow-injection calibration of standard metalloproteins allows for determination of the amount of metal eluting from the column on a per-point basis. The half-peak width of moderately abundant metalloproteins was typically around 20 s, equivalent to approximately 14 points per peak. Integration of the area under curve (AUC) for each peak can feasibly be used to quantify total metal loading on species-specific metalloproteins, adding to available options including quantification *via* isotope-dilution ICP-MS.[33–35]

Diversity in metalloproteins between cell types

Neurons and astrocytes predictably display a diverse range of metalloprotein species (Fig. 2 and 3). The Fe-binding species of neurons and astrocytes were generally comparable, with major Fe-containing peaks observed at approximately V_e/V_0 (ratio of elution volume to void) = 1.55 (M_W = 450 kDa) and V_e/V_0 = 1.84 (M_W = 80 kDa), as well as low mass species eluting after the total column volume (V_T; M_W < 0.5 kDa). As expected, the majority of Fe in both cell types is likely associated with high molecular weight ferritin (V_e/V_0 = 1.55; M_W = 450 kDa), and astrocytes were observed to contain as much as 10 times more ferritin-bound Fe than neurons. Ferritin is ubiquitously expressed in both neurons and astrocytes, the amount of which differs depending on both brain region[36] and Fe homeostatic requirements.[37] The peak at V_e/V_0 = 1.84 (M_W = 80 kDa) is likely to be indicative of the major Fe-transport protein transferrin.

Ceruloplasmin (Cp; V_e/V_0 = 1.74; M_W 151 kDa) accounts for over 90% of circulating Cu and plays a major role in brain Fe metabolism.[38] Interestingly, this protein was observed almost exclusively in neurons (see Fig. 2). Immunohistochemical studies of Cp in brain sections has previously identified expression in both cell types,[39] and it is unclear as to why cultured astrocytes do not display a Cu peak corresponding to Cp. A variety of Cu-binding proteins and peptides have been identified in astrocytes, including transporters (Copper transporter receptor 1 – Ctr1; divalent metal transporter 1 – DMT1; ATP7A), intracellular traffickers (SOD-1, copper chaperone for superoxide dismutase – CSS; ATOX1, Cox17), and storage and detoxifiers (metallothioneins – MTs).[40] Both cell types, though more pronounced in astrocytes, showed colocalised Cu and Zn peaks, reflective of SOD-1 homodimer (see Fig. 3) at V_e/V_0 = 2.02 (M_W = 32 kDa). A common Cu-binding protein is observed in both cell

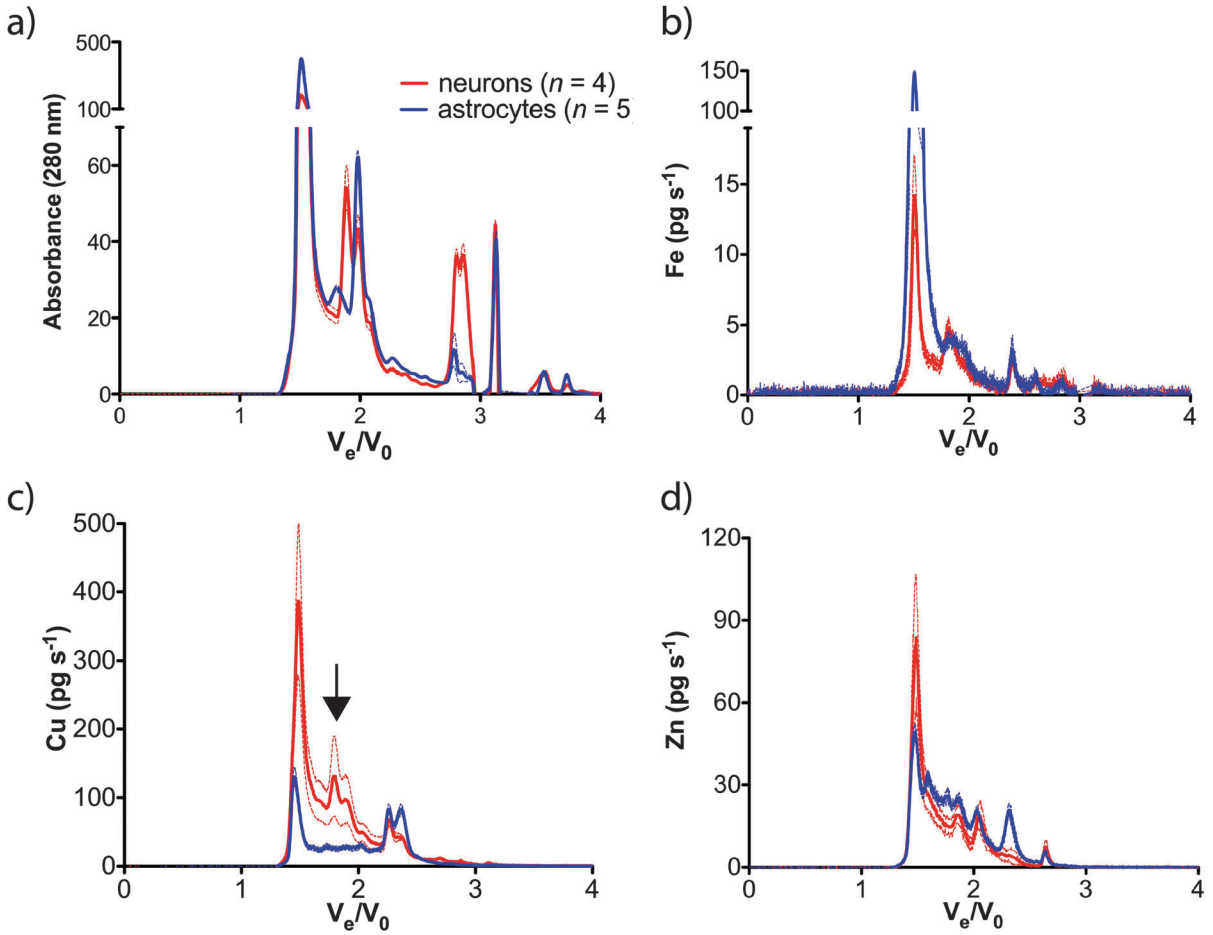

Fig. 2 (a) UV absorbance trace (280 nm), (b) Fe, (c) Cu and (d) Zn chromatograms from neuron (red line) and astrocyte (blue line) cultures. Dashed line = ±1 standard deviation, n = 4 (neurons) and n = 5 (astrocytes). Black arrow denotes Cu-binding Cp (V_e/V_0 = 1.74).

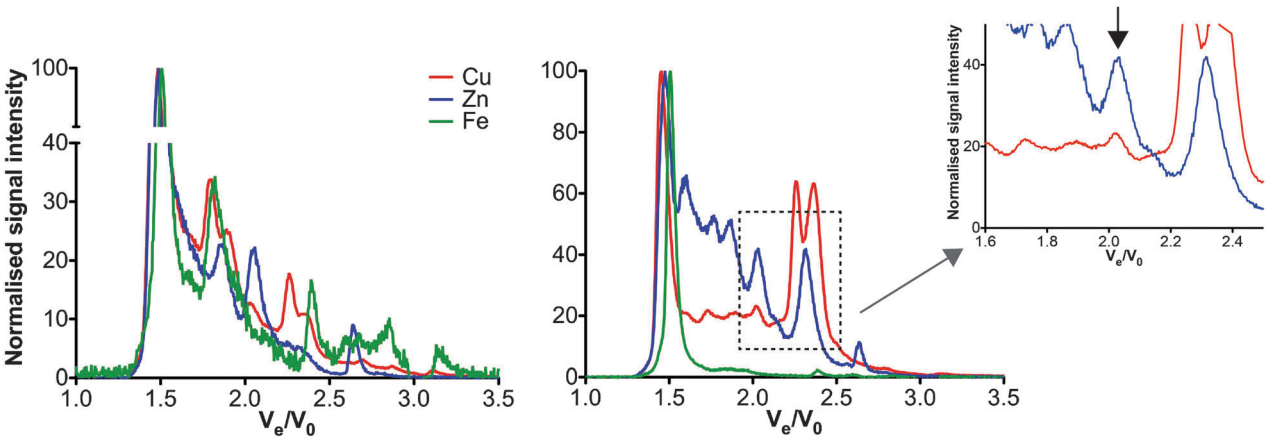

Fig. 3 Overlay of normalised Fe, Cu and Zn traces for cultured neurons (left) and astrocytes (right). Inset: Cu and Zn peak at V_e/V_0 = 2.02 in astrocytes corresponds to SOD-1 homodimer (M_W 32 kDa; black arrow).

types at V_e/V_0 = 2.26 (M_W = 6 kDa) that may be attributable to either MTIIa (per the standard protein) or small cuproproteins, such as Cox17 and ATOX1.[41] An extremely small peak is observed in astrocytes at V_e/V_0 = 1.71 (M_W = 178 kDa) may be indicative of Ctr1.[28]

The Zn profile in both cell types was generally similar, with the exception of a major Zn binding protein at V_e/V_0 = 2.32 (M_W = 4.1 kDa) in astrocytes not identified in neurons. A similar Cu-containing peak at V_e/V_0 = 2.36 (M_W = 3.2 kDa) is also observed in astrocytes. These peaks are thought to represent

astrocytic expression of MT isoforms, which are high affinity Zn (and Cu) binders expressed in this cell type that play an important role in the response to neuronal injury.[42–44] *In situ* hybridization, radioimmunoassay and immunohistochemistry has previously identified MT-I and -II expression in glia and ependymal cell cultures.[45]

Growth conditions of both cell types may influence the metalloprotein profile. Neurons were grown in serum-free Neurobasal medium (following an initial period on serum-containing media), whilst astrocytes were grown in 10% fetal bovine serum. This difference may account for differing protein expression, though this also reflects the different extracellular environments each cell type would maintain *in vivo*. Regardless, growing either cell type in a consistent serum-rich or serum-free environment would only serve to produce unviable cells, which would undoubtedly produce an artificial affect on protein diversity. This approach has greater utility in studying the cellular response to metal dyshomeostasis: further work will examine shifts in metalloprotein species following the addition of bioavailable metals. However, a possible avenue of investigation could use a transient/separable co-culture system (reviewed by Miki *et al.*[46]) in order to expose cells to the same growth media.

Global *versus* targeted metalloproteomics

The typical approach to metalloprotein analysis can best be described as a targeted method, where specific purification and sample cleanup steps precede direct measurement of a known species *via* electrospray MS, such as metallation status of SOD-1 in ALS spinal cord tissue[47,48] and heavy metal-binding MT isoforms in hepatic and renal tissue[49–51] (see Eve Roberts' review[52] for a comprehensive synopsis of targeted metalloproteomic strategies from the perspective of hepatic disorders). The approach described here provides a 'global' evaluation for comparative biology across a broad mass range, which allows for rapid identification of either generalised metal deficiency (as we observed with respect to Fe) or changes in a specific metal-binding peak, which may be a candidate for a more targeted metalloproteomic assay. For specific conditions, such as familial ALS where metallation status of the abundant metalloenzyme is impaired, this approach provides not only sufficient native chromatographic resolution to isolate SOD-1, but also provides an accurate quantification method that can be related to protein–metal stoichiometry. As such, this rapid quantitative technique has the potential to play an important role in the study of disorders involving impairment to metal metabolism.

Conclusions

Primary cultures of murine neurons and astrocytes contain a wide range of metalloproteins, which can be quantified with relative simplicity using native SEC hyphenated to ICP-MS and a range of metalloprotein standards. Native chromatography allows direct detection of metal cofactors in a non-denaturing environment, ensuring that the relatively weak interactions typical of protein–metal complexes are preserved. Online quantitative SEC-ICP-MS extends the capabilities of hyphenated techniques to allow direct detection and quantification of metal cofactors, thus allowing meaningful biological comparison of the role of the metalloproteome in health and disease.

Acknowledgements

Funding for this project was provided by the Australian Research Council, Victorian Government's Operational Infrastructure Support program and National Health and Medical Research Council. We wish to thank Professor Adrian West of the University of Tasmania for providing metallothionein IIa standards.

Notes and references

1 L. Zecca, R. Pietra, C. Goj, C. Mecacci, D. Radice and E. Sabbioni, *J. Neurochem.*, 1994, **62**, 1097–1101.
2 R. R. Crichton, D. T. Dexter and R. J. Ward, *Coord. Chem. Rev.*, 2008, **252**, 1189–1199.
3 B. R. Roberts, T. M. Ryan, A. I. Bush, C. L. Masters and J. A. Duce, *J. Neurochem.*, 2011, **120**, 149–166.
4 D. J. Hare, J. K. Lee, A. D. Beavis, A. van Gramberg, J. George, P. A. Adlard, D. I. Finkelstein and P. A. Doble, *Anal. Chem.*, 2012, **84**, 3990–3997.
5 J. D. Cahoy, B. Emery, A. Kaushal, L. C. Foo, J. L. Zamanian, K. S. Christopherson, Y. Xing, J. L. Lubischer, P. A. Krieg, S. A. Krupenko, W. J. Thompson and B. A. Barres, *J. Neurosci.*, 2008, **28**, 264–278.
6 J.-W. Yang, R. Rodrigo, V. Felipo and G. Lubec, *J. Proteome Res.*, 2005, **4**, 768–788.
7 F. Stellato, A. Spevacek, O. Proux, V. Minicozzi, G. Millhauser and S. Morante, *Eur. Biophys. J.*, 2011, **40**, 1259–1270.
8 P. Giannozzi, K. Jansen, G. L. Penna, V. Minicozzi, S. Morante, G. Rossi and F. Stellato, *Metallomics*, 2012, **4**, 156–165.
9 H. Haraguchi, *J. Anal. At. Spectrom.*, 2004, **19**, 5.
10 A. Lothian, D. J. Hare, R. Grimm, T. M. Ryan, C. L. Masters and B. R. Roberts, *Front. Aging Neurosci.*, 2013, **5**, 35.
11 A. Sanz-Medel, *Spectrochim. Acta, Part B*, 1998, **53**, 197.
12 H. L. Lelie, A. Liba, M. W. Bourassa, M. Chattopadhyay, P. K. Chan, E. B. Gralla, L. M. Miller, D. R. Borchelt, J. S. Valentine and J. P. Whitelegge, *J. Biol. Chem.*, 2011, **286**, 2795–2806.
13 P. E. Gardiner, E. Rosick, U. Rosick, P. Bratter and G. Kynast, *Clin. Chim. Acta*, 1982, **120**, 103.
14 P. E. Gardiner, P. Braetter, B. Gercken and A. Tomiak, *J. Anal. At. Spectrom.*, 1987, **2**, 375–378.
15 B. Gercken and R. M. Barnes, *Anal. Chem.*, 1991, **63**, 283–287.
16 S. F. Boulyga, V. Loreti, J. Bettmer and K. G. Heumann, *Anal. Bioanal. Chem.*, 2004, **380**, 198–203.
17 S. Kameo, K. Nakai, N. Kurokawa, T. Kanehisa, A. Naganuma and H. Satoh, *Anal. Bioanal. Chem.*, 2005, **381**, 1514–1519.
18 J. G. Morrison, P. White, S. McDougall, J. W. Firth, S. G. Woolfrey, M. A. Graham and D. Greenslade, *J. Pharm. Biomed. Anal.*, 2000, **24**, 1.
19 S. A. Manley and J. Gailer, *Expert Rev. Proteomics*, 2009, **6**, 251–265.

20 C. S. Muñiz, J. M. M. Gayón, J. I. G. Alonso and A. Sanz-Medel, *J. Anal. At. Spectrom.*, 2001, **16**, 587–592.
21 M. Schrag, A. Dickson, A. Jiffry, D. Kirsch, H. V. Vinters and W. Kirsch, *Biometals*, 2010, **23**, 1123–1127.
22 B. Todorich, X. Zhang and J. R. Connor, *Glia*, 2011, **59**, 927–935.
23 J. R. Liddell, D. Obando, J. Liu, G. Ganio, I. Volitakis, S. San Mok, P. J. Crouch, A. R. White and R. Codd, *Free Radical Biol. Med.*, 2013, **60**, 147–156.
24 P. S. Donnelly, A. Caragounis, T. Du, K. M. Laughton, I. Volitakis, R. A. Cherny, R. A. Sharples, A. F. Hill, Q. X. Li, C. L. Masters, K. J. Barnham and A. R. White, *J. Biol. Chem.*, 2008, **283**, 4568–4577.
25 C. Duncan, L. Bica, P. J. Crouch, A. Caragounis, G. E. Lidgerwood, S. J. Parker, J. Meyerowitz, I. Volitakis, J. R. Liddell and R. Raghupathi, *Metallomics*, 2013, **5**, 700–714.
26 G. M. Bishop, T. N. Dang, R. Dringen and S. R. Robinson, *Neurotoxic. Res.*, 2010, **19**, 443–451.
27 J. Riemer, H. H. Hoepken, H. Czerwinska, S. R. Robinson and R. Dringen, *Anal. Biochem.*, 2004, **331**, 370–375.
28 I. F. Scheiber, J. F. B. Mercer and R. Dringen, *Neurochem. Int.*, 2010, **56**, 451–460.
29 S. A. Bellingham, G. D. Ciccotosto, B. E. Needham, L. R. Fodero, A. R. White, C. L. Masters, R. Cappai and J. Camakaris, *J. Neurochem.*, 2004, **91**, 423–428.
30 C. T. Sheline, T. Takata, H. Ying, L. M. T. Canzoniero, A. Yang, S. P. Yu and D. W. Choi, *Glia*, 2004, **46**, 18–27.
31 G. G. Mackenzie, M. P. Zago, C. L. Keen and P. I. Oteiza, *J. Biol. Chem.*, 2002, **277**, 34610–34617.
32 C. Ferrarello, M. R. Fernández de la Campa and A. Sanz-Medel, *Anal. Bioanal. Chem.*, 2002, **373**, 412–421.
33 T. Konz, M. Montes-Bayon and A. Sanz-Medel, *Anal. Chem.*, 2012, **84**, 8133–8139.
34 I. Konz, B. Fernández, M. L. Fernández, R. Pereiro and A. Sanz-Medel, *Anal. Bioanal. Chem.*, 2012, **403**, 2113–2125.
35 T. Konz, E. Añón-Alvarez, M. Montes-Bayón and A. Sanz-Medel, *Anal. Chem.*, 2013, **85**, 8334–8340.
36 S. A. Benkovic and J. R. Connor, *J. Comp. Neurol.*, 1993, **338**, 97–113.
37 J. Han, J. R. Day, J. R. Connor and J. L. Beard, *J. Nutr.*, 2002, **132**, 2769–2774.
38 V. Desai and S. G. Kaler, *Am. J. Clin. Nutr.*, 2008, **88**, 855S–858S.
39 Y.-W. Li, L. Li and J.-Y. Zhao, *Neurosci. Bull.*, 2008, **24**, 13–20.
40 I. F. Scheiber and R. Dringen, *Neurochem. Int.*, 2013, **62**, 556–565.
41 K. M. Davies, D. J. Hare, V. Cottam, N. Chen and L. Hilgers, *Metallomics*, 2013, **5**, 43–51.
42 R. S. Chung, P. A. Adlard, J. Dittmann, J. C. Vickers, M. I. Chuah and A. K. West, *J. Neurochem.*, 2003, **88**, 454–461.
43 I. Miyazaki, M. Asanuma, H. Hozumi, K. Miyoshi and N. Sogawa, *FEBS Lett.*, 2007, **581**, 5003–5008.
44 I. Miyazaki, M. Asanuma, Y. Kikkawa, M. Takeshima, S. Murakami, K. Miyoshi, N. Sogawa and T. Kita, *Glia*, 2010, **59**, 435–451.
45 B. A. Masters, C. J. Quaife, J. C. Erickson, E. J. Kelly, G. J. Froelick, B. P. Zambrowicz, R. L. Brinster and R. D. Palmiter, *J. Neurosci.*, 1994, **14**, 5844–5857.
46 Y. Miki, K. Ono, S. Hata, T. Suzuki, H. Kumamoto and H. Sasano, *J. Steroid Biochem.*, 2012, **131**, 68–75.
47 T. W. Rhoads, N. I. Lopez, D. R. Zollinger, J. T. Morré, B. L. Arbogast, C. S. Maier, L. DeNoyer and J. S. Beckman, *Anal. Biochem.*, 2011, **415**, 52–58.
48 T. W. Rhoads, J. R. Williams, N. I. Lopez, J. T. Morré, C. S. Bradford and J. S. Beckman, *J. Am. Soc. Mass Spectrom.*, 2013, **24**, 115–124.
49 K. Das, V. Jacob and J. M. Bouquegneau, *Comp. Biochem. Physiol., Part C: Toxicol. Pharmacol.*, 2002, **131**, 245–251.
50 H. Chassaigne and R. Lobinski, *Analyst*, 1998, **123**, 2125–2130.
51 H. Chassaigne and R. Łobiński, *J. Chromatogr., A*, 1998, **829**, 127–136.
52 E. A. Roberts, *Metallomics*, 2012, **4**, 633.

